Internet of Things Infrastructure Based on Fast, High Spatial Resolution, and Wide Measurement Range Distributed Optic-Fiber Sensors

Shuai Qu, Zequn Wang, Zengguang Qin, Yanping Xu, Zhenhua Cong, and Zhaojun Liu

***Abstract*—Information sensor can realize the ubiquitous connection between objects and humans by the distributed fiber-optic sensor array, i.e., emerging infrastructure for Internet of Things, in which optical frequency domain reflectometry (OFDR) with its high spatial resolution plays an important role in achieving intelligent perception and identification of the objects. However, given a certain fiber length, there are tradeoffs among the processing speed, the spatial resolution, and the strain measurement range. In this article, a time optimization interpolation method and a distance domain compensation method are reported and experimentally verified to break the aforementioned tradeoffs for the first time. First, a full theoretical analysis on how to reduce the interpolation number and the reason why it is difficult to achieve high spatial resolution and large strain measurement and how to resolve it is made. Second in the proof-of-concept experiment, measurements of large strains up to 10 000 $\mu\varepsilon$ are realized along the sensing fiber with a spatial resolution of 2 mm using a conventional OFDR system. Also, the processing time is shortened by 76 times compared with the traditional processing method. This article makes a significant step toward high-performance OFDR system with fast processing, high spatial resolution, and wide strain measurement.**

***Index Terms*—Fiber optics sensors, Internet of Things (IoT), optical frequency domain reflectometry (OFDR).**

I. Introduction

THE Internet of Things (IoT) is an expanded network based on the Internet, which aims at realizing the interconnection between objects and humans via combining various information sensor devices with the Internet [1]. Everything could be intelligently sensed, recognized, and managed by a sensing device that connects through the IoT to form a huge network. That is to say, electronic sensors are now playing a primary role in connecting the objects and humans. WiFi, mobile cellular networks, and Bluetooth have been applied as a tool to transmit large amounts of data for human's intelligent identification. However, limited by the capabilities of wireless channels, the data transmission of the IoT is still a huge challenge for smarter world [2]. In addition, numerous electronic sensors need to be deployed, which is a time-consuming and laborious task. In order to overcome those problems, the distributed optical fiber sensing technique provides a potential for information transmission and sensors deployment in IoT [3]. Optical fiber shows the most powerful information transmission capability, through which large amounts of sensing data can be easily transmitted [4]–[7]. In distributed optical fiber sensing, optical fiber itself as an effective sensing array can be viewed as a collection of a massive number of virtual sensors. Thus, a large number of information sensors are deployed once the sensing fiber is laid [3]. Temporal and spatial mapping of the environmental quantities, such as temperature, vibration, and strain can be detected by the optical fiber sensing technology [8], [9]. In addition, power supply is not required for each sensor, thus ensuring high energy efficiency in distributed optical fiber sensing. Compared with the traditional electronic counterpart, optical fiber sensors are not limited by the signal bandwidth as the information of each sensor is extracted from the backscattered lights sharing the same bandwidth. Also, the distributed optical fiber sensing technique provides a promising alternative to electronic sensors, benefitted from their distinct advantages of high detection sensitivity, fast response, resistance to electromagnetic interference, and low cost owing to the characteristics of optical fiber materials [10]. The phase-sensitive optical time-domain reflectometry (φ-OTDR)-based distributed optic-fiber sensing technique has been employed to help build up the smart city by measuring the acoustic wave and vibration [3]. However, this technology has limited spatial resolution on the order of meters due to the wide pulse width. In addition, most state-of-the-art φ-OTDR systems are developed for dynamic measurements such as vibration by extracting amplitude variation of signals within a given period of time instead of static measurements, in which signal amplitude remains almost unchanged over a given period of time, including the strain and temperature, which are key parameters in the health monitoring of object structures. Thus, developing a new distributed optical fiber sensing technology to realize

Manuscript received February 27, 2021; revised May 6, 2021 and June 16, 2021; accepted June 29, 2021. Date of publication July 2, 2021; date of current version February 4, 2022. This work was supported in part by the Natural Science Foundation of Shandong Province under Grant ZR2020MF110 and Grant ZR2020MF118; in part by the Shandong Provincial Key Research and Development Program (Major Scientific and Technological Innovation Project) under Grant 2020CXGC010204; and in part by the Qilu Young Scholar Program of Shandong University. *(Shuai Qu and Zequn Wang contributed equally to this work.) (Corresponding author: Zhaojun Liu.)*

Shuai Qu, Zequn Wang, Zengguang Qin, Zhenhua Cong, and Zhaojun Liu are with the School of Information Science and Engineering and the Shandong Provincial Key Laboratory of Laser Technology and Application, Shandong University, Qingdao 266237, China (e-mail: qushuai@mail.sdu.edu.cn; 201932511@mail.sdu.edu.cn; qinzengguang@sdu.edu.cn; congzhenhua@sdu.edu.cn; zhaojunliu@sdu.edu.cn).

Yanping Xu is with Center for Optics Research and Engineering, Shandong University, Qingdao 266237, China (e-mail: yanpingxu@sdu.edu.cn).

Digital Object Identifier 10.1109/JIOT.2021.3094272

multiparameter and high spatial resolution measurement is of great significance for the IoT-applications.

The optical frequency domain reflectometry (OFDR) is a sensing system based on swept-wavelength homodyne interferometry [11], which is one of the effective ways to overcome those challenges to replace other sensors for smarter sensing in wide areas, including small mechanical structures and soft machines. Recently, simultaneous scan of multiple sensing fibers is realized by the scattering-level multiplexing (SLMux) technique based on the OFDR system, which can simultaneously monitor fibers arranged in an arbitrary shape so that the sensing network detection system can be built up [12]. The local information can be extracted after the Rayleigh scattering signal is collected as a function of the frequency in a complex fashion and then processed using the fast-Fourier transform so that a distance-domain mapping of the scattering strength as a function of sensing fiber length can be constructed. Changes of the surrounding environment or machine structures can be detected when the sensing fiber is laid on the object under test. Up to now, the OFDR technique has been applied in many fields to achieve strain [13], [14], and vibration sensing [15], [16], temperature [17], [18], and humidity [19], [20], measurement, shape sensing [21], [22], gas sensing [23], [24], and even acoustic sensing [25], [26]. It is able to perceive variations of environmental parameters due to its unique advantages, which is potentially one of the best ways to achieve human-computer interaction.

In the OFDR system, processing speed, spatial resolution, and strain measurement range are the main parameters that are used to evaluate the performance of the system. The processing speed reflects the real-time nature of the system and it largely depends on the data size of the sampling signal. The number of interpolations before the cross-correlation calculation will further influence the processing speed due to the complexity of data processing [27]. The spatial resolution refers to the minimum resolvable spatial length for environmental parameter measurements. It is limited by the sweeping range of the TLS. High spatial resolution can be obtained by improving the sweeping range at the cost of a rapid increase in processing time. The maximum detectable strain measurement range is impacted by the strain-induced stretched length of the sensing fiber, which reduces the similarity between the reference signal and the measurement signal. In cases of large strains, the stretched length is so large that the spatial resolution has to be compromised by increasing the fiber section window length in order to accurately retrieve the real spectrum shift caused by the strain through cross-correlation calculation. Thus, there are always tradeoffs among those parameters in the OFDR system. In order to improve the measurement performance, various optical configurations, and methods have been reported to improve the key parameter of the system. Specifically, the image denoising method and sliding window method are employed to improve the spatial resolution perfectly [28], however, the position deviation of the stretched fiber cannot be resolved and the processing time is significantly increased by several orders. Several effective methods, such as local similar characteristics of the Rayleigh scattering spectrum [29] and spectrum registration [30] are proposed to improve the strain measurement range in OFDR system, and the graphic processing unit (GPU) is introduced to accelerate the speed of signal processing [30]. In contrast, the spatial resolution has to be broadened for achieving wide strain measurement range. Up to now, reports for breaking the above tradeoffs to improve the measurement performance of the OFDR system are infrequent [31]. Thus, asserting a compromise proposal to resolve the tradeoff in the OFDR technique is a pivotal step for its rapid application in smarter detections.

In this article, first, the interpolation method before cross-correlation calculation is discussed and an optimized scheme is shown compared with the traditional processing method in the OFDR system. Then a theoretical analysis for position deviation caused by the wide strain value is derived and the strain measurement range can be improved without sacrificing the spatial resolution. The position deviation is compensated so that spectral shifts caused by large strains are calibrated and extracted to acquire the strain information. Finally, an OFDR system with micron-level spatial resolution and a maximum detectable strain up to ten thousand micro-strain is demonstrated. Due to the advantages of our proposed scheme in OFDR system, the measurement efficiency and energy efficiency are both higher than the conventional electronic sensors. Also, this technique may provide a potential method to resolve the difficulty of applying the distributed optical fiber sensing system for measurements of large strains related to soft robots [10], smart buildings monitoring used for energy and network [32], [33]. Therefore, in the future this technique could replace the traditional sensors and be widely applied in the IoT field for smarter sensing and measurement.

II. Principle

A. Principle of the OFDR System

The OFDR system generates a beat signal which is introduced by the optical interference between two light signals originating from the same linearly frequency chirped highly coherent light source. Fig. 1(a) demonstrates the schematic representation of an OFDR system which is constituted of a TLS, two optical fiber couplers, a circulator, and the sensing fiber for distributed sensing. The beat signal is collected from the interference between the local oscillator signal and the backscattered Rayleigh reflection signal during the period when the laser wavelength is being tuned. In this way, the delay time can be transformed into beat frequency variations, which is subjected to the strain and temperature variations over the sensing fiber. Assuming that the electric fields of the reference signal and the backscattered Rayleigh reflection signal are $E_r(t)$ and $E_b(t)$, respectively, and described as [34]

$$E_r(t) = E_0 \exp\left\{j\left[2\pi f_0 t + \pi\gamma t^2 + \phi(t)\right]\right\} \tag{1}$$

$$E_b(t) = \sqrt{R(\tau)}E_0 \exp\left\{j\left[2\pi f_0(t-\tau) + \pi\gamma(t-\tau)^2 + \phi(t-\tau)\right]\right\} \tag{2}$$

where E_0 is the amplitude of the signal. f_0 is the initial optical frequency of the TLS. γ is the optical frequency tuning speed. τ represents the delay time between the reference light and

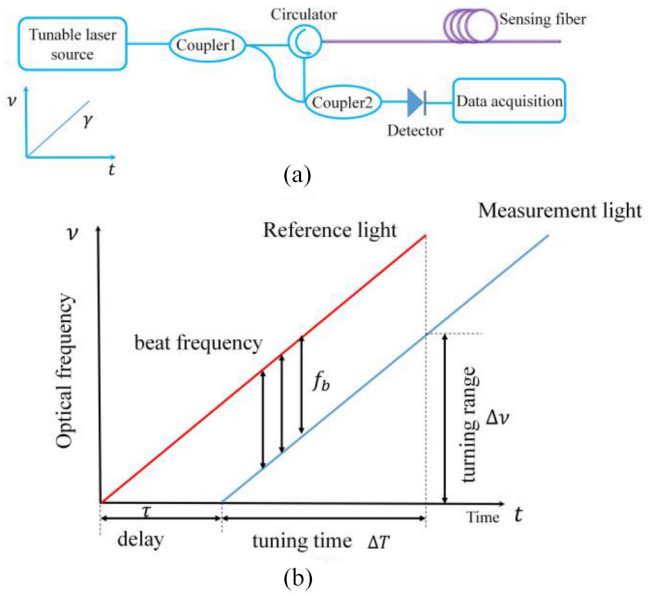

Fig. 1. (a) Schematic representation of a basic OFDR configuration. (b) Optical frequency tuning and the interference between the reference light and the measurement light in ODFR system.

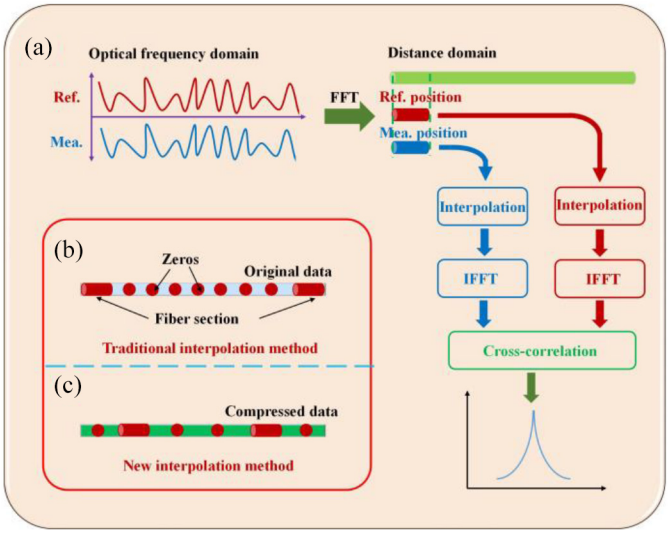

Fig. 2. Data process in the OFDR-based distributed sensing system. (a) Single position processing scheme of the OFDR system. (b) Traditional interpolation method. (c) Proposed interpolation method.

measurement light. $\phi(t)$ and $\sqrt{R}(t)$ represent the phase noise and the reflectivity of the sensing fiber, respectively. Therefore, the beat signal $I(t)$ can be obtained from the interference between the reference light and the measurement light and is given as

$$I(t) = 2\sqrt{R(\tau)E_0^2}\cos \times \left\{2\pi\left[f_0\tau + \gamma\tau t + \frac{1}{2}\gamma\tau^2 + \phi(t) - \phi(t-\tau)\right]\right\}. \quad (3)$$

The term $\phi(t)-\phi(t-\tau)$ represents the phase noise in the beat signal. It can be found in Fig. 1(b) that the beat frequency is proportional to the delay time or the length of the sensing fiber. In OFDR, the beat frequency signal can be written as

$$f_b = \gamma\tau = \frac{2nz\gamma}{c} \quad (4)$$

where z is the length from a certain position along the sensing fiber to the fiber starting point. c and n are the speed of light in vacuum and the effective index of the sensing fiber, respectively.

B. Feasibility Demonstration of the Fast OFDR

To extract the environmental parameter variation information along the sensing fiber, two different states, including the unchanged state and changed state are collected in frequency domain by running the OFDR system twice. The processing procedure of the collected data in OFDR system is demonstrated in Fig. 2(a). The initial interference signal is obtained in the frequency domain by scanning the optical frequency of the TLS, which is then transformed to the distance domain information along the entire fiber length by the fast Fourier transform (FFT). Then a segment of the distance domain data at the same positions from both the reference and measurement profiles is extracted to calculate the variations information along the fiber. After that, the interpolation padding zeros method is applied to expand the data size so as to avoid the deterioration of resolving power of the system. Finally, the local distance domain information is transformed back into the optical frequency domain through the inverse FFT (IFFT), and the spectrum shifts induced by the strain will be acquired by the cross-correlation calculation. Thus, the distributed measurement can be achieved by extracting spectrum shifts along the sensing fiber at all sections in the similar way.

In OFDR, the processing time of the system is proportional with the number of data points after interpolation. The traditional interpolation method is shown in Fig. 2(b). The fiber section that decides the spatial resolution is put at the position where is same with the extraction position. However, since the distance domain information obtained by FFT is symmetrical compared with the optical frequency domain information, the fiber section will also be placed in the mirror position of the extraction position, as shown in Fig. 2(b). After the placement position of the fiber section is determined, the remaining part is filled by the zero padding to the same size as the original data. However, due to the huge amount of data, the processing time of the cross-correlation will be increased greatly in the OFDR system along all the fiber. To solve this problem and to realize the fast OFDR, the placed position of the fiber section is adjusted so that the total data size before cross-correlation can be compressed. For the proposed interpolation method, as shown in Fig. 2(c), the fiber section is placed at a quarter position of the compressed data size. Other positions will also be filled by the zero padding. In this case, the number of the compressed data points can be much smaller than that in the traditional method. Therefore, compared with the traditional interpolation method, the proposed method is able to decrease the processing time and achieve the real-time OFDR as the processing time of cross-correlation calculation is reduced greatly.

C. High Spatial Resolution and Wide Measurement Range OFDR

In OFDR system, in order to realize the distributed measurement along the sensing fiber, the entire sensing fiber in distance domain is divided into hundreds of fiber sections by using a sliding window with a length of l_{sr}, which includes M data points as the spatial local Rayleigh scattering signals. Thus, l_{sr} determines the spatial resolution of OFDR system, which is given by [35]

$$l_{sr} = M\Delta Z \tag{5}$$

with

$$\Delta Z = \frac{c}{2n\Delta\nu} \tag{6}$$

where ΔZ is the spatial resolution of one data point. n and $\Delta\nu$ are the effective index of the sensing fiber and the optical frequency tuning range of TLS, respectively.

However, there is a tradeoff between the spatial resolution and the strain measurement range. To illustrate the impact of the stretch in the Rayleigh-scatter-based OFDR strain sensing system, the schematic diagram of stretched fiber is exhibited in Fig. 3(a). The stretched range of the fiber is shown by the blue and orange color, in which the orange is used to represent the stretched length, while the blue represents the original fiber length without strain. The total stretched range will be increased with large strains, however, it can be found that the similarity of the fiber at the stretched position is different with the different spatial resolution and it is inversely proportional to the spatial resolution. In other words, the strain information may be hardly to be distinguished with high spatial resolution due to the spatial mismatch caused by the large stretched length. To show the error results caused by the spatial mismatch vividly, Fig. 3(b)–(d) give the cross-correlation results of measurements with different strain values. When the fiber is unstrained, as shown in Fig. 3(b), the peak of the cross-correlation is overlapped with the central peak and there is no spectrum shift due to the high similarity between the reference signal and measurement signal. In Fig. 3(c), when a weak strain is applied on the sensing fiber, there is still some similarity between the reference signal and the measurement signal, thus, the cross-correlation peak will be away from the center peak. When the strain is large enough, as shown in Fig. 3(d), the spatial mismatch will become more obvious as the stretch length and spatial resolution are increased. The spectral peak shift may be obtained if there is some similarity between the two signals, as shown by the red dotted line. Meanwhile, the degradation of the similarity will cause the fake peaks so that the real shift cannot be extracted, as shown by the blue solid line. In addition, the large strain may result in the spatial mismatch of the sensing fiber after the stretched position for high spatial resolution measurement, and the correct variation information cannot be obtained along the sensing fiber.

According to the above analysis, the measurement of large strain with high spatial resolution, especially in the micron level, remains a great challenge. To overcome this problem, the conception of the Rayleigh scattering center point is introduced to represent the position deviation at the distance

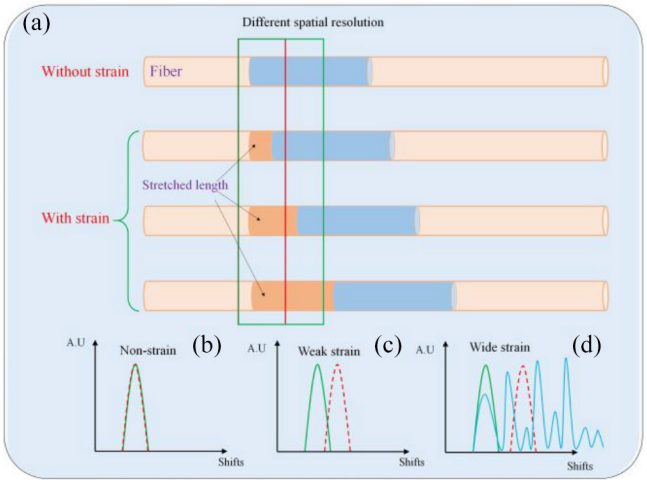

Fig. 3. Strain measurement principle of the distributed OFDR system. (a) Difference between the static and stretched state of the sensing fiber, in which the orange color represents the stretched length of the fiber. (b)–(d) Show the spectrum shifts with different strain state after cross-correlation. (b) Nonstrain. (c) Weak strain state. (d) Wide strain.

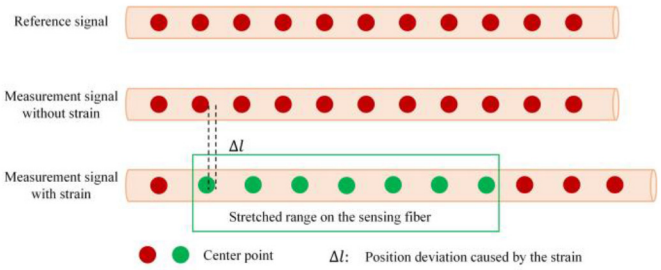

Fig. 4. Distributed Rayleigh scattering center point shift at distance domain between the reference signal and measurement signal with and without strain.

domain. As shown in Fig. 4, along the all position of the sensing fiber, theoretically, each section of the reference signal and measurement signal data points has the same corresponding center point with any spatial resolution when the fiber is not stretched by the strain. However, the center point will be shifted gradually in the distance domain due to the stretch until the strain is too large to be recognized. Thus, to compensate the stretched length of the sensing fiber for calibration, the center point position shifts compensation scheme is an ideal method to improve the similarity between the reference signal and measurement signal, especially in large strain range and high spatial resolution distributed OFDR measurement.

The logical process of the principle of the distance domain compensation method in OFDR is shown in Fig. 5. The fiber section which is used to determine the distributed spatial resolution is selected in the distance domain. It is noted that the center point at the first position on the sensing fiber is the same between the reference signal and the measurement signal. Then the cross-correlation spectral shift is calculated by the scheme shown in Fig. 2(a). At this moment, the shift is the spectrum shift rather than the position deviation which is caused by the strain. Thus, a transformation should be conducted between the spectrum shift and position deviation. To obtain the position deviation, the strain degree which is defined

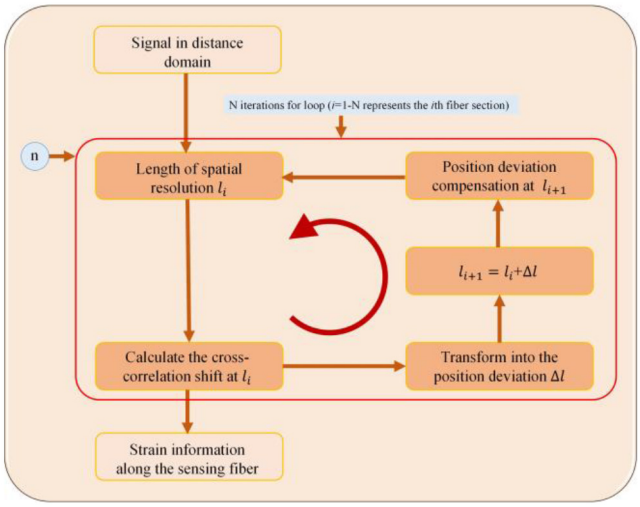

Fig. 5. Logical process principle of position deviation to obtain the high spatial resolution and wide strain range distributed sensing.

as a change of one micron for a length of 1 m is introduced so that the position deviation is expressed as follows:

$$\Delta l = \frac{S_{\text{shift}} \times l_{\mu\varepsilon}}{l_{sr}} \tag{7}$$

where Δl is the position deviation in distance domain. S_{shift} represents the spectrum shift caused by the strain. $l_{\mu\varepsilon}$ is the strain degree. The next fiber section $i+1$, therefore, is compensated by Δl. Finally, the distributed strain information along the sensing fiber is obtained by repeating the above process until the last fiber segment.

III. Experimental Results and Discussion

A. Experimental Setup for Distributed Sensing

The experimental setup of the OFDR-based strain sensing system is shown in Fig. 6. Light from a narrow linewidth continuous TLS (TLS, Agilent 81960A) through an optical isolator (ISO) is split into two parts by a coupler (OC1, 10/90), in which one is sent to the main interferometer which is applied to detect the Rayleigh scattering information, and the other one is sent to the auxiliary interferometer which is used to provide an external clock signal to correct the nonlinear tuning errors of the swept laser that would otherwise adversely affect the collected data. The main output of TLS is sent into the main interferometer and then it is separated into two sections by a 1/99 optical coupler (OC2), in which the 99% of the light is sent into the sensing fiber through a circulator (CIR) and a polarization controller (PC2), and the other section is launched into PC1 for adjusting the polarization of the local path to have the same power for "*p*" and "*s*" components. The beat signal is generated in OC3 by mixing the local signal and the Rayleigh scattering signal, which is then split into "*p*" and "*s*" components by a polarization beam splitter (PBS) and detected by the balanced photodetector (PD, Thorlabs, PDB-450C). Finally, the "*p*" and "*s*" components are collected by the data acquisition (DAQ, NI-6115) card. The rest output from OC1 is injected into the auxiliary interferometer, an imbalanced Mach–Zehnder trigger interferometer to provide

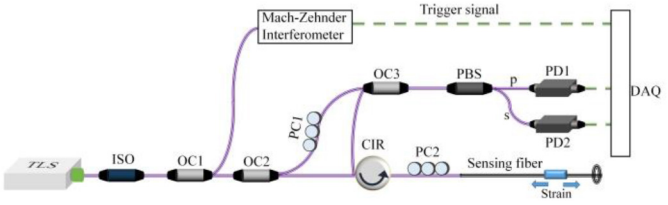

Fig. 6. Experiment setup of OFDR-based strain-sensing system. TLS: tunable laser source; ISO: optical isolator; OC: optical coupler (OC1:10:90, OC2: 1:99 OC3: 50:50); PC: polarization controller; CIR: circulator; PBS: polarization beam splitter; PD: photodetector; and DAQ: data acquisition.

the trigger signal to DAQ. At the end of the sensing fiber, a small circle is made to reduce the Fresnel reflection.

For the OFDR system, the maximum length of the sensing fiber is determined by the differential delay in the auxiliary interferometer based on the Nyquist sampling criteria [36]. It can be expressed as

$$L_m = \frac{c\tau}{4n} \tag{8}$$

where c is the velocity of light in vacuum. τ represents the delay introduced by the auxiliary interferometer. n is the index of the sensing fiber.

B. Experimental Results

In OFDR, the sweep rate of TLS is $\gamma = 40$ nm/s and the turning range is 40 nm (from 1530 to 1570 nm), which corresponds to a total laser sweeping time of 1 s. The length of path difference in the auxiliary interferometer is 50 m so that the sampling rate and the maximum measurable range are 1.25 M/s and 12.5 m, respectively. The probe light via the circulator is launched into the standard single-mode fiber with a total length of about 11.2 m. Then, after setting the experiment parameters, a static state signal is collected as the reference signal for detecting the spectrum shifts induced by the strain variations. The distance domain information which includes the Rayleigh backscattering information as a function of sensing fiber length after vector summing from the "*s*" and "*p*" components is shown in Fig. 7(a) and the detailed characteristic information along the sensing fiber can be obtained. It can be found that there are three obvious peaks in Fig. 7(a), in which the first two peaks are introduced by the reflections from two pairs of angled physical contact connectors and the last peak is caused by the reflection of the end circle of the sensing fiber.

To assess the performance of large strain detection using the distributed measurement system, a translation stage is applied to stretch the sensing fiber with a section length of about 0.3 m at the end of the fiber to provide different strains in the OFDR system. Strains ranging from 1000 to 10 000 $\mu\varepsilon$ with an increment of 1000 $\mu\varepsilon$ are applied on the sensing fiber and collected one by one by the DAQ card. It is noted that the parameters of the east test are the same as those when we measured the reference signal. After collecting the strain information, the experimental data is processed with a 2 mm spatial resolution by the traditional processing method. The detailed information of the strain without distance domain compensation is shown in Fig. 7(b). It can be found that the

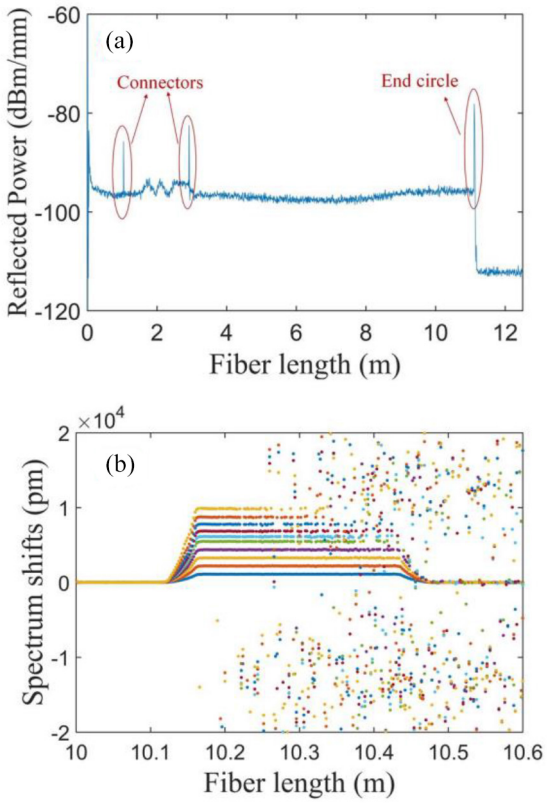

Fig. 7. (a) Distance domain information of the reference signal with nonstrain of the OFDR system. The first two peaks are introduced by the APC-APC connection and the last peaks are caused by the small circle fiber. (b) Result of the conventional processing method based on cross-correlation calculation.

strain profiles will be much more difficult to be identified when the strain is increased, which is due to the spatial mismatch between the reference signal and the measurement signal. In addition, it could be seen that the spatial mismatch will influence the information identification of the fiber state after the strain position when the strain is large, at this moment, many outliers are observed along the sensing fiber.

C. Discussion and Realized the Wide Strain Distributed OFDR Measurement

Before realizing the large strain distributed OFDR measurement, the influence of spatial mismatch which is caused by the large strain on the similarity of the spectrum between the reference signal and measurement signal is discussed by using a large strain of 10 000 $\mu\varepsilon$ as an example. The local reference spectrum and the measurement spectrum information at different positions along the sensing fiber are shown in Fig. 8. It is found in Fig. 8(a) that there is high similarity and repeatability between the reference spectrum and the measurement spectrum when the position is before the fiber stretched position, thus, there is no spectrum shift after the cross-correlation, as shown in Fig. 7(b). However, when the fiber is stretched by a large strain, degradation of similarity between the reference signal and measurement signal is observed in Fig. 8(b) so that maybe the correct strain information is not acquired due to the spatial mismatch. For the position after the stretched

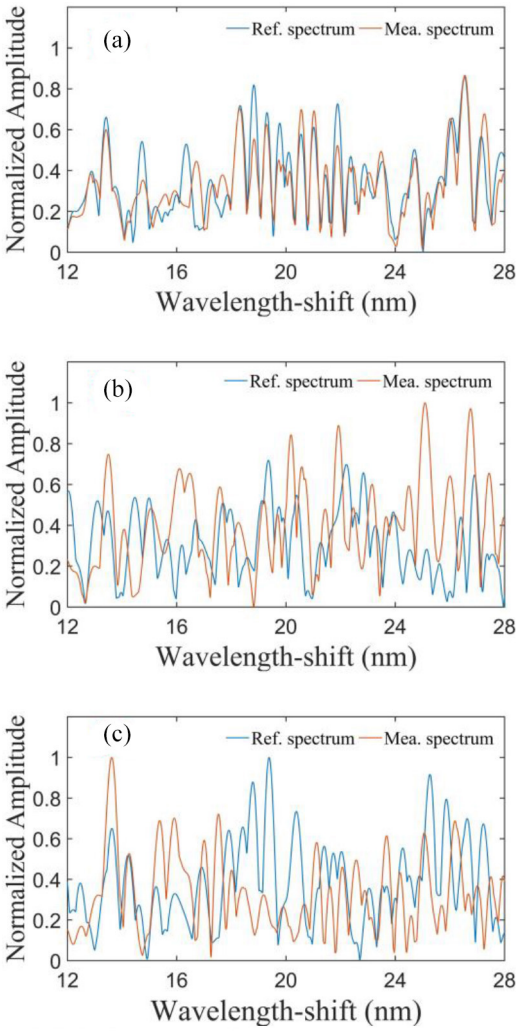

Fig. 8. Similarity between the reference spectrum and measurement spectrum at different position along the sensing fiber. (a) 10.1 m. (b) 10.4 m. (c) 10.5 m.

range, as shown in Fig. 8(c), it is also found that the similarity of the spectrum is reduced. This is because the distance domain length of the measurement signal is stretched and it no longer corresponds to the position of the reference signal. Therefore, it is hardly to recognize the large strain information along the sensing fiber by the traditional method.

In order to compensate the length of the spatial mismatch to realize the large strain measurement in OFDR, the distance domain compensation is proposed by calculating the length using (5). The length deviation of the $i+1$th measuring point is corrected by the spectrum shift value of the ith point. Fig. 9(a) shows the compensation result with 2 mm spatial resolution by using the scheme in Fig. 5. In Fig. 9(a), it can be found that the strain gradient information is identified clearly and outlies caused by the strain are removed by the proposed method. Also, the fake peaks are eliminated at the measured positions after the stretched area. Therefore, the result with distance domain compensation is highly robust and correct. In addition, the linear relationship and linear fitting between the implemented strain and the frequency shifts obtained by the proposed method is shown in Fig. 9, in which the black

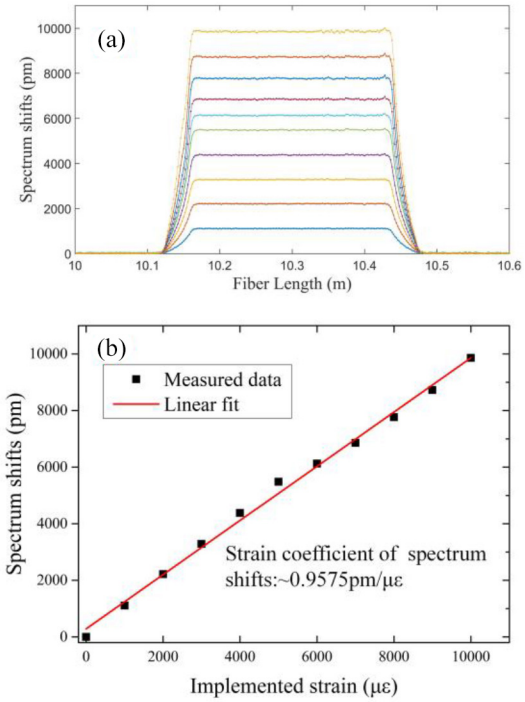

Fig. 9. Strain information along the sensing fiber obtained by the proposed method. (a) Demodulation results calculated by the distance domain position deviation compensation. (b) Linear relationship between the implemented strain and the spectrum shifts.

TABLE I
PERFORMANCE COMPARISON BETWEEN THE PROPOSED METHOD AND TRADITIONAL METHOD

Method	Cycle number	Data size	Total time
Traditional method	5500	1.25M	1515s
Proposed method	5500	10k	20s

squares represent the measured value and the red line represents the linear fit curve. It is found that there is a good linear relationship between the strain value and the spectrum shift. The results obtained by the proposed method show the feasibility of distance domain compensation for correcting the spatial mismatch caused by the large strain. Compared with the traditional method, this method has the ability to resolve the error caused by the deviation of the stretched position of the sensing fiber and realize large strain measurement in the OFDR system.

D. Comparison Processing Time Between the Proposed Interpolation Method and the Traditional Method

To more clearly compare the performance between the proposed interpolation method and the traditional method, several main parameters, including cycle number, the size of data, and the total proposing time are listed in Table I. It is found in Table I that the data size and the total time required in the proposed method are much smaller than the traditional method. The total time is improved by about 76 times by the new method compared with the traditional method. Therefore, the proposed method has the most potential for real-time measurements by using FPGA and DSP in practice. It should be noted that the same original data and computer are used for the above comparison.

IV. CONCLUSION

In conclusion, in order to realize the fast, high spatial resolution and wide strain measurement range distributed optic-fiber sensors, the interpolation method and distance domain compensation method are used in the OFDR system. The interpolation number before cross-correlation is optimized to improve the processing time, which is shortened by about 76 times compared with that in the traditional method. Errors caused by large strains are analyzed theoretically. The distance domain compensation method is proposed to realize high spatial resolution and wide strain measurement in distributed OFDR system. The proof-of-concept experiment shows that measurements of strains up to ten thousand micron-strain with a micron level spatial resolution are realized along the sensing fiber. Compared with the traditional method, the proposed method has the ability to improve the performance of the OFDR to expand the application areas, such as soft robots and IoT sensing field.

REFERENCES

[1] J. A. Stankovic, "Research directions for the Internet of Things," *IEEE Internet Things J.*, vol. 1, no. 1, pp. 3–9, Feb. 2014.
[2] A. Zanella, N. Bui, A. Castellani, L. Vangelista, and M. Zorzi, "Internet of Things for smart cities," *IEEE Internet Things J.*, vol. 1, no. 1, pp. 22–32, Feb. 2014.
[3] Z. Wang *et al.*, "Distributed acoustic sensing based on pulse-coding phase-sensitive OTDR," *IEEE Internet Things J.*, vol. 6, no. 4, pp. 6117–6124, Aug. 2019.
[4] N. J. Lindsey, T. C. Dawe, and J. B. Ajo-Franklin, "Illuminating seafloor faults and ocean dynamics with dark fiber distributed acoustic sensing" *Science*, vol. 366, no. 6469 pp. 1103–1107, 2019.
[5] D. M. Chow, Z. Yang, M. A. Soto, and L. Thevenaz, "Distributed forward Brillouin sensor based on local light phase recovery," *Nat. Commun.*, vol. 9, pp. 1–9, Jul. 2018.
[6] C. Pang *et al.*, "Opto-mechanical time-domain analysis based on coherent forward stimulated Brillouin scattering probing," *Optica*, vol. 7, no. 2, pp. 176–184, 2020.
[7] D. Zhou *et al.*, "Single-shot BOTDA based on an optical chirp chain probe wave for distributed ultrafast measurement," *Light. Sci. Appl.*, vol. 7, pp. 1–11, Jul. 2018.
[8] M. A. Soto, J. A. Ramirez, and L. Thevenaz, "Intensifying the response of distributed optical fiber sensors using 2D and 3D image restoration," *Nat. Commun.*, vol. 7, Mar. 2016, Art. no. 10870.
[9] Y. Lu, T. Zhu, L. Chen, and X. Bao, "Distributed vibration sensor based on coherent detection of phase-OTDR," *J. Lightw. Technol.*, vol. 28, no. 22, pp. 3243–3249, Nov. 15, 2010.
[10] H. Bai, S. Li, J. Barreiros, Y. Tu, C. Pollock, and R. Shepherd, "Stretchable distributed fiber-optic sensors," *Science*, vol. 370, no. 6518, pp. 848–852, 2020.
[11] M. Froggatt and J. Moore, "High-spatial-resolution distributed strain measurement in optical fiber with Rayleigh scatter," *Appl. Opt.*, vol. 37, no. 10, pp. 1735–1740, 1998.
[12] D. Tosi, C. Molardi, W. Blanc, T. Paixao, P. Antunes, and C. Marques, "Performance analysis of scattering-level multiplexing (SLMux) in distributed fiber-optic backscatter reflectometry physical sensors," *Sensors*, vol. 20, no. 9, p. 2595, 2020.
[13] W. Li, L. Chen, and X. Bao, "Compensation of temperature and strain coefficients due to local birefringence using optical frequency domain reflectometry," *Opt. Commun.*, vol. 311, pp. 26–32, Jan. 2013.

[14] C. Wang *et al.*, "High sensitivity distributed static strain sensing based on differential relative phase in optical frequency domain reflectometry," *J. Lightw. Technol.*, vol. 38, no. 20, pp. 5825–5836, Oct. 15, 2020.
[15] S. Qu *et al.*, "Distributed fiber vibration sensing with single-shot measurement and moving time-gating method," *Opt. Commun*. vol. 47, Nov. 2020, Art. no. 126053.
[16] S. Qu *et al.*, "Distributed sparse signal sensing based on compressive sensing OFDR," *Opt. Lett.*, vol. 45, no. 12, pp. 3288–3291, 2020.
[17] Y. Cheng, M. Luo, J. Liu, and N. Luan, "Numerical analysis and recursive compensation of position deviation for a sub-millimeter resolution OFDR," *Sensors*, vol. 20, no. 19, p. 5540, 2020.
[18] J. Song, W. Li, P. Lu, Y. Xu, L. Chen, and X. Bao, "Long-range high spatial resolution distributed temperature and strain sensing based on optical frequency-domain reflectometry," *IEEE Photon. J.*, vol. 6, no. 3, Jun. 2014, Art. no. 6801408.
[19] P. Thmoas and J. Hellevang, "A high response polyimide fiber optic sensor for distributed humidity measurements," *Sens. Actuators B, Chem.*, vol. 270, pp. 417–423, Oct. 2018.
[20] P. Stajanca, K. Hicke, and K. Krebber, "Distributed fiber optic sensor for simultaneous humidity and temperature monitoring based on polyimide-coated optical fibers," *Sensors*, vol. 19, no. 23, p. 5279, 2020.
[21] C. Shao *et al.*, "OFDR with local spectrum matching method for optical fiber shape sensing," *Appl. Phys. Exp.*, vol. 12, no. 8, 2019, Art. no. 082010.
[22] R. G. Duncan *et al.*, "High-accuracy fiber-optic shape sensing," in *Proc. SPIE*, 2007, Art. no. 65301S.
[23] X. Lou, C. Chen, Y. Feng, and Y. Dong, "Simultaneous measurement of gas absorption spectra and optical path lengths in a multipass cell by FMCW interferometry," *Opt. Lett.*, vol. 43, no. 12, pp. 2872–2875, 2018.
[24] X. Lou, Y. Feng, C. Chen, and Y. Dong, "Multi-point spectroscopic gas sensing based on coherent FMCW interferometry," *Opt. Exp.*, vol. 28, no. 6, pp. 9014–9026, 2018.
[25] T. Okamoto, D. Iida, and H. Oshida, "Vibration-induced beat frequency offset compensation in distributed acoustic sensing based on optical frequency domain reflectometry," *J. Lightw. Technol.*, vol. 37, no. 18, pp. 4896–4901, Sep. 15, 2019.
[26] J. Li *et al.*, "High spatial resolution distributed fiber strain sensor based on phase-OFDR," *Opt. Exp.*, vol. 25, no. 22, pp. 27913–27922, 2017.
[27] J. Cui, S. Zhao, D. Yang, and Z. Ding, "Investigation of the interpolation method to improve the distributed strain measurement accuracy in optical frequency domain reflectometry systems," *Appl. Opt.*, vol. 57, no. 6, pp. 1424–1431, 2018.
[28] S. Zhao, J, Cui, Z. Wu, and J. Tan, "Accuracy improvement in OFDR-based distributed sensing system by image processing," *Opt. Laser Eng.*, vol. 124, Jan. 2020, Art. no. 105824.
[29] K. Peng *et al.*, "Improvement of the strain measurable range of an OFDR based on local similar characteristics of a Rayleigh scattering spectrum," *Opt. Lett.*, vol. 43, no. 14, pp. 3293–3296, 2018.
[30] S. Zhao, J. Cui, L. Suo, Z. Wu, D.-P. Zhou, and J. Tan, "Performance investigation of OFDR sensing system with a wide strain measurement range," *J. Lightw. Technol.*, vol. 37, no. 15, pp. 3721–3727, Aug. 1, 2019.
[31] (2020). *Data Sheet of ODISi-6000*. [Online]. Available: https://lunainc.com/wp-content/uploads/2017/11/LUNA-ODiSI-6000-Data-Sheet.pdf
[32] C. K. Metallidou, K. E. Psannis, and E. A. Egyptiadou, "Energy efficiency in smart buildings: IoT approaches," *IEEE Access*, vol. 8, pp. 63679–63699, 2020.
[33] C. L. Stergiou, K. E. Psannis, and B. B. Gupta, "IoT-based big data secure management in the fog over a 6G wireless network," *IEEE Internet Things J.*, vol. 8, no. 7, pp. 5164–5171, Apr. 2021.
[34] K. Feng *et al.*, "Investigation of a signal demodulation method based on wavelet transformation for OFDR to enhance its distributed sensing performance," *Sensors*, vol. 19, no. 13, p. 2850, 2019.
[35] Z. Ding *et al.*, "Distributed optical fiber sensors based on optical frequency domain reflectometry: A review," *Sensors*, vol. 18, no. 4, pp. 1–31, 2018.
[36] B. J. Soller, D. K. Gifford, M. S. Wolfe, and M. E. Froggatt, "High resolution optical frequency domain reflectometry for characterization of components and assemblies," *Opt. Exp.*, vol. 13, no. 2, pp. 666–674, 2005.